Inductorless Synchronized Switch Harvesting Using a Piezoelectric Oscillator

Mickael Lallart, Wen-Jong Wu, Linjuan Yan, Sheng-Wei Hung

Inductorless Synchronized Switch Harvesting using a Piezoelectric Oscillator

Mickaël LALLART, Wen-Jong WU, Linjuan YAN and Sheng-Wei HUNG

The present manuscript has neither been presented at a conference nor submitted elsewhere previously

Abstract

This paper proposes a preliminary investigation of a voltage inversion technique for enhancing the conversion abilities and power output of piezoelectric energy harvesting systems without requiring any inductance. Based on the use of an additional, decoupled high-frequency piezoelectric oscillator that is intermittently switched on the main harvesting piezoelectric element, the proposed scheme allows obtaining an inversion effect up to 30% experimentally (and possibly much higher) in an inductorless fashion. Such a concept is both discussed and validated theoretically and experimentally. Applied to energy harvesting, this provides an experimental gain of 30% in terms of harvested power compared to short-circuit switching. Also, the proposed scheme can be implemented in a single stage using off-the-shelf components (although being possibly integrated as well) while providing a better management of the charge transfer compared to pure switched capacitance approach thanks to the motional branch of the oscillator. This therefore enables low-cost, integrable power boosting technique for piezoelectric vibrational energy harvesters.

Index Terms

Energy harvesting, Piezoelectric devices, Piezoelectric transducers, Switched circuits.

M. Lallart and L. Yan are with the Univ. Lyon, INSA-Lyon, LGEF EA 682, F-69621, VILLEURBANNE, FRANCE (M. Lallart, LGEF INSA-Lyon, 8, rue de la Physique, 69621 VILLEURBANNE Cedex, FRANCE / e-mail: mickael.lallart@insa-lyon.fr / ORCID $0000-0002-6907-5946$); W.-J. Wu is with the Department of Engineering Science and Ocean Engineering, National Taiwan University, No. 1, Sec. 4, Roosevelt Road, Taipei, 10617 Taiwan (R.O.C) and the Univ. Lyon, INSA-Lyon, LGEF EA 682, F-69621,, VILLEURBANNE, FRANCE (e-mail: wjwu@ntu.edu.tw / ORCID $0000-0003-0223-249X$) ; S.-W. Hung is with the Department of Engineering Science and Ocean Engineering, National Taiwan University, No. 1, Sec. 4, Roosevelt Road, Taipei, 10617 Taiwan (R.O.C).

I. INTRODUCTION

The spreading of wireless autonomous sensors, for instance in the framework of "Internet of Things" concept, has raised the issue of ensuring power supply in applications where the device is barely accessible or faces relatively harsh environmental conditions. Indeed, in such a case, the use of conventional chemical batteries may not be satisfactory due to the self-discharge of such elements that is even more pronounced with relatively high temperatures for instance ([1–3]) with possible safety issues ([4]). Hence, in order to provide alternative solutions, the concept of "Energy Harvesting", consisting in converting surrounding energy source into electricity, has been proposed since more than two decades ([5–9]).

Among the potential energy sources available in the typical surroundings of target applications (for instance solar and thermal), mechanical energy through vibrations is particularly attractive as the latter are widely available even in confined environments. Hence, many works were devoted to this kind of energy source, including power conditioning circuit aspects ([10]). In this area, many works aim at developing maximum power extraction from the transducers. This includes Maximum Power Point Tracking strategies ([11]) and optimal voltage tracking systems ([12, 13]). Low voltage input, especially when rectification is required, is also an issue widely addressed in literature ([14–17]), as well as low-power interface ([18]). In a small-scale view, the use of piezoelectric effect is also of premium interest as such materials show high integration potentials as well as high power densities. Nevertheless, the conversion abilities of such vibration piezoelectric energy harvesters (VPEH) are still limited by the relatively low coupling coefficient of cost-affordable materials or integrated materials, as well as the mechanical quality factor of the structure. In order to artificially increase such conversion abilities, another class of circuits has been under investigation, mostly relying on nonlinear electrical interface. More precisely, the Synchronized Switch Harvesting on Inductor (SSHI) technique ([19–22]), along with its derivatives (Double/Enhanced Synchronized Switch Harvesting - [23, 24] -, SSHI-MR - [25] -, SECE and O-SECE - [26–28] - or Synchronous Inversion and Charge Extraction - [29] - for instance), have been proved to be an efficient way for magnifying the power generation performances of VPEHs. Such an enhancement originates from the principles of the Synchronized Switch which consist of inverting the output voltage of the piezoelectric element when the latter reaches an extremum value, through a brief connection to an inductance (thus shaping a resonant electrical network together with the natural capacitive electrical behavior of the piezoelement). Such an inversion allows both a cumulative amplification process of the piezoelectric voltage magnitude as well as a reduction of the phase shift between voltage and velocity, with these two effects contributing to the conversion ability magnification.

Nevertheless, as piezotransducer dimensions shrink ([30, 31]), electrical interfaces should also show reduced size. Hence, efforts in material integration should be accompanied with electronic interface integration as well ([15–18, 32]). In the case of the SSHI however, the critical component lies in the inductance used for the inversion process. While the value of the latter is quite limited, especially compared to passive tuning ([33]), it is typically chosen around $1 - 100$ mH in practical implementation ([34]), so that switching losses do not significantly compromise the inversion. Hence, with integration objective in mind, only Synchronized Switch techniques without the use of such an inductive component show significant integration potentials, such as SSHS (Synchronized Switch Harvesting

on Short Circuit, which is similar to the SSHI approach but without inversion effect - [20, 21]) or SSDC ([35])[1] techniques, which however yields a degradation in terms of energy harvesting performance. To address this issue, some implementations of the Synchronized Switch Harvesting using capacitor to capacitor charge transfer have been proposed to keep part of the benefit brought by the inversion effect. More specifically, Chen et al. ([36, 37]) proposed to use a reconfigurable capacitor array (allowing parallel, series or parallel/series hybrid arrangement of the capacitors) to manage charge transfer, hence achieving significant inversion ($> 80\%$) resulting in 3.4 gain in terms of harvested power compared to non-switched case, at the cost of complex switching array and control. Closer to the SSHI principles, Du and Seshia used conventional switched capacitor topology in order to perform the inversion ([34]). Consisting in 1) charge transfer from the piezoelectric element to a passive capacitor; 2) piezoelectric charge cancellation and 3) Charge transfer from the (reversed) capacitor to the piezoelectric element, along with capacitor charge recycling from one inversion event to another, the single-stage implementation yielded an inversion efficient of 33% for a single stage (25% without capacitor residual charge recycling). In this work, the extension to multiple stage was also demonstrated, where a 8-stage interface being able to achieve inversion of 80% (equivalent performance than SSHI with a 5.6 mH inductor in the considered case). Yet, intrinsic losses of capacitor to capacitor direct charge transfer require multiple stages as well as microelectronic implementation which might not be economically viable when considering that energy harvesting devices target a relatively small market at the present time.

Hence, in order to dispose of an inductorless, single-stage inversion circuit using off-the-shelf components, the present study proposes to replace the switched capacitance by a secondary, possibly smaller (compared to the global transducing structure), independent piezoelectric element as an oscillator. This permits taking advantage of the motional branch of this element (that can be modeled in the electronic point of view as a RLC circuit) that naturally allows, thanks to the mechanical oscillation arising from the electromechanical coupling, a voltage inversion effect if the coupling is high, or enhance the inversion compared to the pure switched capacitance strategy (for the same number of stages). The paper is organized as follows. Section II aims at providing the basics of such a proposed approach, named SSHO for "Synchronized Switch Harvesting on Oscillator", as well as the theoretical analysis, whose results are preliminary discussed in Section III. Then in order to experimentally validate the concept, Section IV proposes some preliminary practical implementation and performance analysis together with comparison with theoretical predictions. Finally, Section V briefly recalls the main findings of this study as well as future enhancements such as multi-stage integration.

II. PRINCIPLES AND ANALYSIS

A. Synchronized Switch Harvesting on Oscillator (SSHO) concept

The principles of the inductorless SSH, namely the Synchronized Switch Harvesting on Oscillator (SSHO) lies in replacing the inductance (SSHI) or the switching capacitance (SSHC) by a piezoelectric oscillator, yielding the circuit and equivalent representation depicted in Fig. 1. Hence, compared to switched capacitor-based inversion

[1]SSDC technique being possibly viewed as series SSHI without inductance - [21]

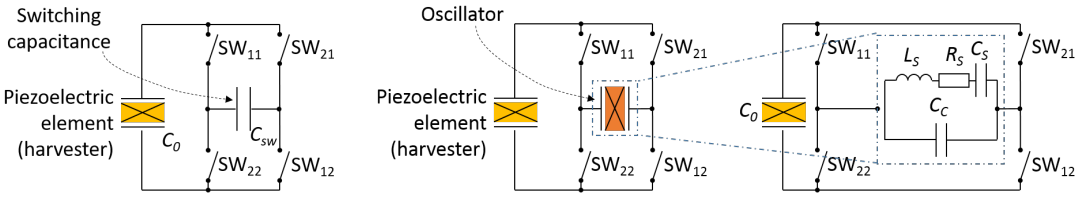

(a) Switched capacitor (b) SSHO

Fig. 1. Principles of single-stage a) conventional switched capacitance and b) inductorless synchronized switch.

techniques, the motional branch of the oscillator permits benefiting of an supplementary oscillation that actually allows magnifying the inversion process. In other words, such an approach enables the transformation of the capacitance used in switched capacitor techniques into an active component, with the kinetic energy tank being played by the dynamic mass of the oscillator rather than an inductance (in the conventional SSHI case).

The circuit operations are as follows. When the harvester voltage reaches either a minimum or maximum value, switches SW_{11} and SW_{12} are closed. This first yields a charge transfer/neutralization from the harvester capacitance C_0 to the clamped capacitance of the oscillator (C_C), corresponding to step (1) in the waveforms illustrated in Fig. 2. Once this almost instantaneous discharge completed, the motional branch is excited yielding oscillations (step (2) in Fig. 2). After half a pseudo-period of such oscillations, the connection polarity of the oscillator is reversed, by opening switches SW_{11} and SW_{12} and closing SW_{21} and SW_{22}. This re-initiate a similar process, with at first charge neutralization between C_0 and C_C (step (3) in Fig. 2) and oscillation of the motional branch in parallel with C_0 and C_C (step (4) in Fig. 2). Again, the switches are re-openened after half a pseudo-period, which terminates the inversion process. Hence, compared to pure capacitor switching, the mechanical oscillation of the oscillator permits further reducing the voltage (steps 2 and 4 in Fig. 2), therefore enabling a better inversion effect, or reducing the number of required stages.

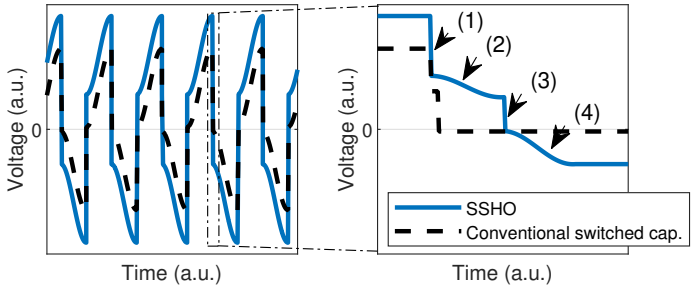

Fig. 2. Voltage waveform example and comparison with conventional switched capacitor (for the latter case only steps (1) and (3) - *i.e.*, charge neutralization - occur).

B. Theoretical analysis

The present section aims at evaluating the voltage inversion efficiency with respect to the piezoelectric element voltage at the beginning of the process, noted V_0, and circuit parameters (piezoelectric clamped capacitance C_0, oscillator clamped capacitance C_C and oscillator motional branch parameters, namely inductance L_S, resistance R_S and capacitance C_S). For the sake of simplicity and to focus more on the SSHO concept, only one inversion stage will be considered throughout this paper, and with no intermediate charge neutralization (such possibilities being addressed in further works together with integration issues).

1) First charge neutralization: For the first step, only transfer of charges from the piezoelectric harvester to the clamped capacitance of the oscillator occurs, and the motional branch does not intervene as the inductance first prevents current flowing. Hence, assuming that the oscillator initial voltage is null (oscillator is totally discharged since last inversion because of damped mechanical oscillations), and considering charge balance before and after this first process, the expression of the voltage V_1 after this charge transfer yields:

$$V_1 = \frac{C_0}{C_0 + C_C} V_0 \tag{1}$$

2) First oscillation: Then, the second step consists in the first oscillation of the motional branch. From the equivalent circuit analysis (Fig. 1), this leads to the following differential equation:

$$-L_S C_{eq} \ddot{V}_p + R_S C_{eq} \dot{V}_p + V_p = \frac{C_0 + C_C}{C_0 + C_C + C_S} V_1 \tag{2}$$

where V_p is the harvester voltage and $C_{eq} = \frac{(C_0+C_C)C_S}{C_0+C_C+C_S}$. Terminating this oscillation after a time period $t_2 = \pi\sqrt{L_S C_{eq}}$ (half of the oscillation pseudo period) gives the voltage value V_2 as:

$$V_2 = \left(\frac{C_0 + C_C - \gamma C_S}{C_0 + C_C + C_S} \right) V_1 \tag{3}$$

with:

$$\gamma = \exp\left(-\pi \frac{\xi_0}{\sqrt{1 - {\xi_0}^2}} \right) \tag{4}$$

where ξ_0 refers to the damping ratio of the global system (harvester + oscillator):

$$\xi_0 = \frac{1}{2} R_S \sqrt{\frac{C_{eq}}{L_S}} \tag{5}$$

Also, the voltage V_{S2} across the motional branch capacitance C_S at the end of this process is given by:

$$V_{S2} = \left(\frac{C_0 + C_C}{C_0 + C_C + C_S} \right) (1 + \gamma) V_1 \tag{6}$$

3) Second charge neutralization: Once the first half pseudo-period terminated, switches SW_{11} and SW_{12} are opened while SW_{21} and SW_{22} are closed. Hence, the oscillator polarity is reversed and another charge neutralization occurs between C_0 and C_C leading to the voltage after step (3) (with respect to Fig. 2):

$$V_3 = \frac{C_0 - C_C}{C_0 + C_C} V_2 \tag{7}$$

4) Second oscillation stage: Once this second charge neutralization occurred (in an almost instantaneous way), the oscillator is again excited. However, during this second process a residual charge remains on the oscillator motional branch capacitance as defined in (6). Hence, the governing differential equation is therefore given by:

$$-L_S C_{eq} \ddot{V}_p + R_S C_{eq} \dot{V}_p + V_p = \frac{(C_0 + C_C) V_3 - C_S V_{S2}}{C_0 + C_C + C_S} \tag{8}$$

yielding the fourth and last voltage expression, V_4:

$$V_4 = \frac{(C_0 + C_C - \gamma C_S) V_3 - (1+\gamma) C_S V_{S2}}{C_0 + C_C + C_S} \tag{9}$$

Combining (9), (7), (6), (3) and (1) therefore leads to the expression of the voltage V_4 after the inversion process as a function of the voltage V_0 before the inversion process as:

$$V_4 = \frac{(C_0 - C_C)(C_0 + C_C - \gamma C_S)^2 - (1+\gamma)^2 (C_0 + C_C)^2 C_S}{(C_0 + C_C)^2 (C_0 + C_C + C_S)^2} C_0 V_0 \tag{10}$$

Introducing the ratio x between the clamped capacitances as well as the coupling coefficient k of the oscillator (assuming low losses - *i.e.*, $\xi_0 \ll 1$) as:

$$\begin{cases} x &= \frac{C_C}{C_0} \\ k^2 &= \frac{C_S}{C_C + C_S} \end{cases} \tag{11}$$

leads to the following reduced expression of the final voltage V_4 as a function of the initial one, V_0:

$$V_4 = \frac{(1-x)\left[1 + x - k^2 - (1+\gamma) k^2 x\right]^2 - \left(1 - k^2\right)(1+\gamma)^2 (1+x)^2 x k^2}{(1+x)^2 (1 + x - k^2)^2} V_0 \tag{12}$$

Hence, the inversion factor $\Gamma = -V_4 / V_0$ yields:

$$\Gamma = \frac{\left(1 - k^2\right)(1+\gamma)^2 (1+x)^2 x k^2 - (1-x)\left[1 + x - k^2 - (1+\gamma) k^2 x\right]^2}{(1+x)^2 (1 + x - k^2)^2} \tag{13}$$

III. THEORETICAL DISCUSSION

Voltage inversion value obtained from theoretical analysis ((12) and (13)) is depicted in Fig. 3 as a function of clamped capacitance ratio as well as electromechanical coupling of the oscillator for several values of the quality coefficient γ (defined in (4)). Results confirm that the proposed approach permits benefiting from a voltage inversion effect without the use of an inductance thanks to the use of the oscillator. However, inversion effect can only be obtained for a particular value of the oscillator capacitance which depends on the coupling coefficient. In addition,

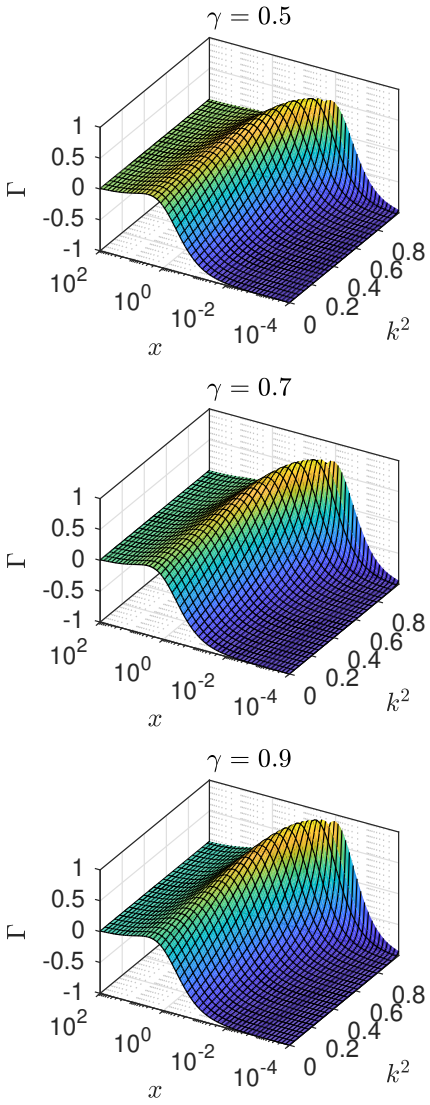

Fig. 3. Inversion factor as a function of capacitance ratio and oscillator coupling.

compared to the case of pure switched capacitors ($k^2 = 0$) the electromechanical coupling, represented by the motional branch of the oscillator, allows a significant magnification of the inversion.

Such an effect can be also observed by plotting the maximal inversion factor as a function of the electromechanical coupling coefficient as depicted in Fig. 4. Hence, for high coupling coefficients, this permits a significant gain (up to 7) of the inversion factor. This Figure also clearly shows that the global quality factor (through the value of γ) of the oscillator influences the inversion factor, with an increased performance for lower losses. Finally, it can be noted that the optimal clamped capacitance ratio, namely x_{opt}, decreases as the oscillator electromechanical coupling increases but does not vary significantly with γ.

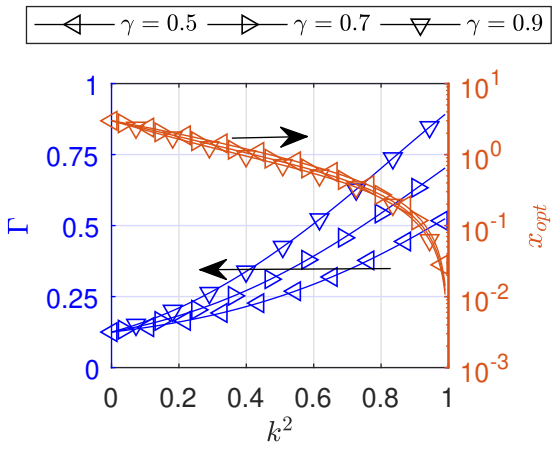

Fig. 4. Optimal operations as a function of squared coupling coefficient of the oscillator.

A. *Comparison with switched capacitor inverter (SSHC)*

The principles of the SSHO consist of making the pure capacitance of switched capacitor inverter (SSHC - [34]) electromechanically active in order to dispose of a kinetic energy tank (*i.e.*, dynamic mechanical mass of the oscillator) to further improve the inversion efficiency. Hence, considering single stage inversion as in the present study, the SSHC cannot go beyond an inversion factor of 0.33, while in the case of the SSHO the inversion can be theoretically ideal ($\Gamma = 1$ - however in practical implementation the value can be expected lower considering the limitations in terms of coupling factor and damping of the oscillator) even with only one stage. However, one advantage of the SSHC is the fact that the charges on the passive capacitors can be kept from one inversion event to the other one, while for the SSHO, the mechanical damping would likely yield zero initial conditions for the oscillator at each inversion event occurrence.

Furthermore, in the previously exposed concept, no piezoelectric voltage cancellation occurs (between steps (2) and (3) in Fig. 2) as in the SSHC. Actually, this would even further enhance the inversion factor (however, such a charge cancellation step is out of the scope of the present study that primarily aims at exposing the SSHO concept). Meanwhile, for the SSHC scheme, not implementing the charge cancellation step would yield a maximal inversion factor of 25% ([34]). Hence, further implementations of the SSHO, including multi-stage inversion and

Technique	Condition	Inversion coefficient
SSHC Single stage	$C_C = C_0$, zero initial charge on C_C, no losses considered	25%
SSHC Single stage	$C_C = C_0$, charges on C_C kept, no losses considered	33%
SSHC 5 stages	$C_C = C_0$, charges on C_C kept, no losses considered	71%
SSHO Single stage	$C_C = 0.6C_0$, $k^2 = 0.6$, $\gamma = 0.7$, no charge neutralization	38%
SSHO Single stage	$C_C = 0.25C_0$, $k^2 = 0.8$, $\gamma = 0.9$, no charge neutralization	70%

TABLE I

COMPARISON BETWEEN SSHC AND SSHO.

charge cancellation, would permit a significant enhancement for inductorless inversion, or, for the same inversion coefficient, a reduced number of required stages. As an example, Table I shows that, for relatively well-coupled oscillator, the single stage SSHO can perform as well as 5-stage SSHC. Furthermore, it should be noted that the SSHC inversion factor has been computed without considering charge transfer losses, which might yield decreased performance in terms of inversion capabilities, especially when considering off-the-shelf implementation.

Table II shows more detailed performance comparison between the proposed circuit topology and other state-of-the-art interface designs. Comparing with other inductor-based designs, the proposed architecture allows eliminating such bulky components as well as associated generated electromagnetic field which may cause electromagnetic interference (EMI). Similar inductorless topologies used to realize charge transfer and achieve voltage inversion, called FCR (*"Flipping-Capacitor Rectifier"* - [36, 37]) and SSHC (*"Synchronized Switch Harvesting on Capacitors"* - [34]), the voltage flipping efficiency in this work is lower than previous mentioned topologies. However Table I shows that the proposed scheme can have outstanding performance by choosing a well-coupled and suitable oscillator without charge neutralization step according to simulation results. From this result, we also find out performance improvement considering either charge neutralization step and/or multi-stage architecture as shown in Table , although the latter approach is out of the scope of this paper and only given as preliminary results. The SSHO-1 (for single stage) provides up to 6.6x and 6.1x boost, respectively with and without charge neutralization, yielding power gains more than two times higher than the passive SSHC-1 counterpart.

IV. EXPERIMENTAL VALIDATION

In order to validate the previous developments, this section proposes to experimentally implement the SSHO and investigate its performance.

A. Set-up and characterization

The experimental set-up, depicted in Fig. 5, consists of one dual channel function generator with one channel connected to a shaker through a power amplifier, and the other channel giving the triggering signal for the switching device. This signal is fed to a second dual channel function generator, each channel controlling a pair of switches. The switching device, depicted in Fig. 5(b), consists in two NMOS transistors (2N7000) controlled through an optocoupler. For this preliminary experimental validation of the SSHO concept, the switches are externally powered using a stabilized power supply. The piezoelectric element, in addition to the connection to the switching circuit, can also be connected to a voltage doubler rectifying interface. Finally, voltage outputs of the piezoelectric element and switch control are monitored through an oscilloscope.

Prior to experimental measurements in the framework of the present study, characterization of the oscillator has been made using a network analyzer (Agilent Technology E5061B). Obtained response around the first resonance frequency is given in Fig. 6, along with the theoretical curve obtained from the equivalent circuit model whose fitted parameters are listed in Table III. Finally, the clamped capacitance of the harvester has been measured to be equal to 20.5 nF.

B. Experimental results

Considering the previously exposed device without the harvesting stage, a successful inversion effect has been observed as shown in Fig. 7. Results therefore show an inversion factor of $\Gamma = 0.23$, close to the theoretical value of 0.21 (as $x = 0.53$ and $k^2 = 32\%$). Nevertheless, in order to further investigate the proposed scheme and validate the theoretical development, extra capacitances have been added to the piezoelectric element acting as harvester to vary the oscillator to harvester capacitance ratio. When considering that the microgenerator can be modeled

Reference	**Technique**	**Transducer**	**Piezo cap.**	**Freq.**	**Inductor**	**Capacitor**	**Power Extraction Improvement**	**Voltage Flipping Efficiency (Steady-State)**	**Voltage Flipping Efficiency (1st Inversion)**
JSSC 2010 [A]	P-SSHI	Mide V22B	18 nF	225 Hz	47uH	N/A	4x	75%	N/A
JSSC 2016 [B]	P-SSHI	Mide V21&22B	9.6nF	225Hz	3.3mH	N/A	6.81x	94%	N/A
TCAS-I 2017 [C]	P-SSHI	Mide V22B	19nF	144Hz	220uH	N/A	2.07x	75%	N/A
JSSC 2017 [D]	FCR	Piezo P5A4E	0.08nF	110kHz	N/A	1.44nF	4.83x	85%	N/A
JSSC 2017 [E]	SSHC-1 SSHC-8	Mide V21BL	45nF	92Hz	N/A	1*45nF 8*45nF	2.7x 9.7x	33% 80%	25% 33%
This Work	SSHO-1 (w/o neutralization)	Custom MEMS	20.5nF	125Hz	N/A	N/A	6.1x	23.4%	20.4%
This Work	SSHO-1 (w/ neutralization)	Custom MEMS	20.5nF	125Hz	N/A	N/A	6.6x	40.6%	42.9%
This Work	SSHO-2 (w/o neutralization)	Custom MEMS	20.5nF	125Hz	N/A	N/A	10.7x	52.5%	47.1%
This Work	SSHO-2 (w/ neutralization)	Custom MEMS	20.5nF	125Hz	N/A	N/A	10.6x	57.9%	52.3%

TABLE II

PERFORMANCE COMPARISON WITH STATE-OF-THE-ART INTERFACE CIRCUITS.

Parameter	Value
Clamped capacitance C_C	10.8 nF
Motional inductance L_S	763 μH
Motional resistance R_S	3.09 Ω
Motional capacitance C_S	5.12 nF

TABLE III

OSCILLATOR LUMPED PARAMETERS.

as a velocity-controlled current source I with a capacitive internal impedance C_0 as (note that in this study, the electromechanical coupling of the harvester is considered low enough not to induce significant mechanical damping effect):

$$I = \alpha \dot{u} - C_0 \dot{V}_P \tag{14}$$

where u refers to the cantilever beam tip displacement (relative to the base), V_P the piezovoltage and α denotes the force factor, adding an extra capacitance C in series or parallel yields an equivalent piezoelectric element with the following modified parameters ($\alpha|_{ser}$ and $\alpha|_{para}$ refer to the equivalent force factors in series and parallel connection respectively and $C_0|_{ser}$ and $C_0|_{para}$ to the clamped capacitances in series and parallel connection respectively):

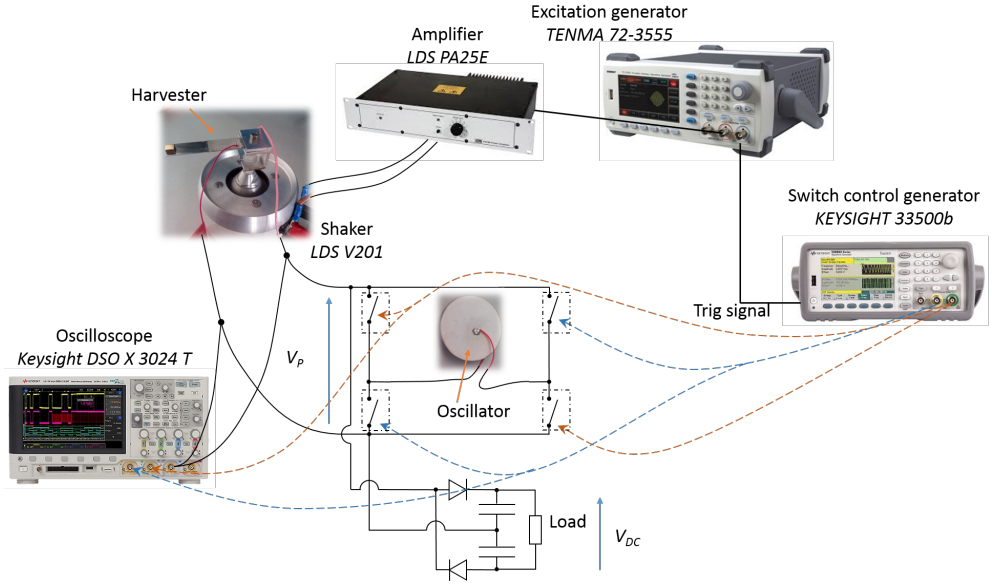

(a) Overview

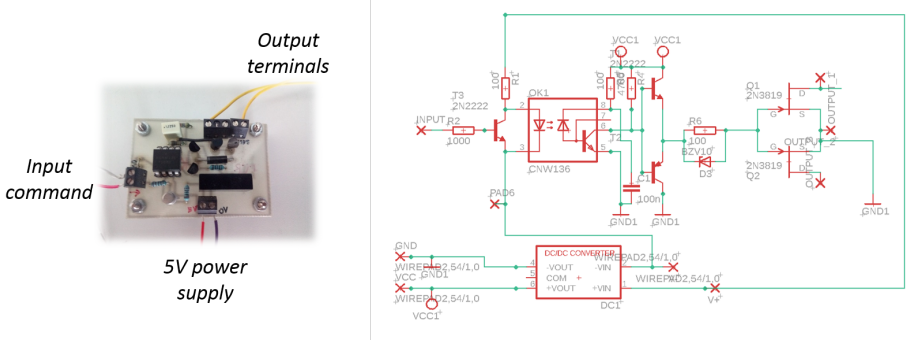

(b) Switching circuit

Fig. 5. Experimental set-up.

$$\begin{aligned} \alpha|_{ser} &= \tfrac{C}{C_0+C}\alpha \\ C_0|\,ser &= \tfrac{C_0 C}{C_0+C} \quad \text{(series configuration)} \end{aligned} \tag{15}$$

$$\begin{aligned} \alpha|_{para} &= \alpha \\ C_0|\,para &= C_0 + C \quad \text{(parallel configuration)} \end{aligned}$$

This addition of a capacitance therefore permits making the capacitance ratio x varying. Varying this ratio is more relevant than modifying the coupling coefficient k of the oscillator as this latter parameter can only be decreased which would yield decreased performance (Fig. 4), while for the parameter x, an optimal value actually exists (Fig. 3). Hence, when doing so, the measured inversion coefficient, along with theoretical predictions, is depicted in Fig. 8. It can be seen from both theoretical and experimental results, that show good agreement, that the inversion can be further maximized in series case with an optimal value around $C = 17$ nF. However, it should be kept in mind that such a series capacitance decreases the conversion efficiency of the piezoelectric element (as denoted by the decreased value of the force factor in (15). In the considered case, the parallel connection does not show any enhancement and eventually leads to a negative inversion coefficient, meaning that the voltage does not change it sign, and therefore underperforms compared to the short circuit switch case (SSHS - Synchronized Switch Harvesting on Short circuit).

C. Application to Energy Harvesting

As the present study is performed in the framework of energy harvesting, this section aims at evaluating the performance of the SSHO. More specifically, the technique is compared to the SSHS case that features similar integration potentials. Note that the equivalent purely capacitive inversion through switched capacitor ($k^2 = 0$) is

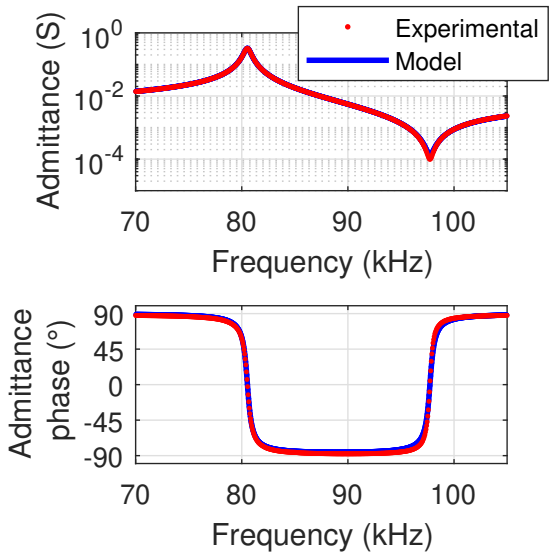

Fig. 6. Oscillator characterization.

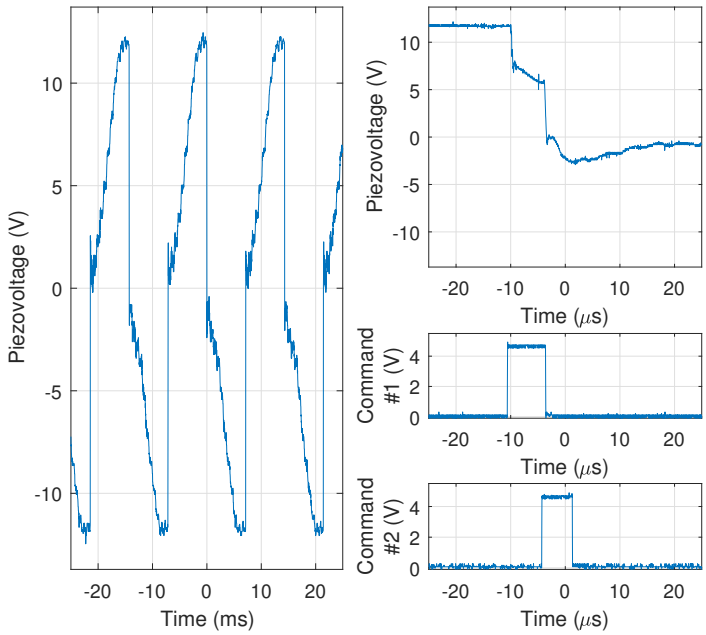

Fig. 7. Experimental waveforms.

not considered in the following as replacing the oscillator by a capacitance with the same value as C_C would yield a negative inversion factor (and therefore would perform worse than SSHS). Considering the transducer without extra capacitance in series or parallel and with the voltage doubler rectifier presented in Fig. 5(a), it can be shown that the harvested power P as a function of the load R is given by:

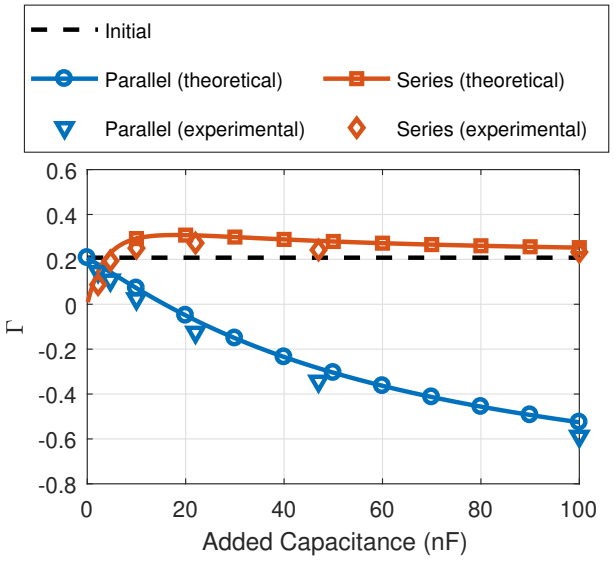

Fig. 8. Inversion factor with varying capacitance.

$$P = \frac{(4\alpha f)^2 R}{[2 + (1 - \Gamma) R C_0 f]^2} {u_M}^2 \tag{16}$$

where $\Gamma = 0$ in the SSHS case and with f denoting the vibration frequency.

For the considered system, the force factor was determined from the displacement magnitude measurement (using a Panasonic HG-C1050-P laser sensor) and open circuit voltage magnitude and has been found to be equal to 0.29 mN.V^{-1}. With a measured displacement magnitude of 710 μm, obtained results in terms of harvested power are depicted in Fig. 9. Experimentally measured harvested powers show good agreement with theoretical ones, demonstrating that the use of a potentially integrable oscillator may advantageously replace inductance to perform inversion effect and thus magnified power compared to short circuit switching, with in this case a power gain of 30% compared to the SSHS technique.

V. CONCLUSION AND FURTHER WORKS

In the framework of integrating electrical interfaces along with the transducing material for energy harvesting devices, this paper exposed a first proof-of-concept of an inductorless approach for performing the inversion of the voltage output of piezoelectric elements in the view of using Synchronized Switch scheme. Unlike conventional switched capacitor approaches that use purely electric components, it has been shown through this study that using a piezoelectric oscillator allows, thanks to its motional branch, significantly magnifying the inversion abilities, and therefore the harvested energy from the microgenerator, even with a single stage considered for this first proof-of-concept validation. As in the case of switched capacitors, further works will consider combining several branches (multiple stage inversion) as well as charge cancellation step of the harvester for further increasing the inversion capabilities (Fig. 10), as well as the integration of the global circuit including the oscillator. To do so, homemade devices can be considered, such as the piezoelectric materials developed by some of the authors (Fig. 11 - [30]).

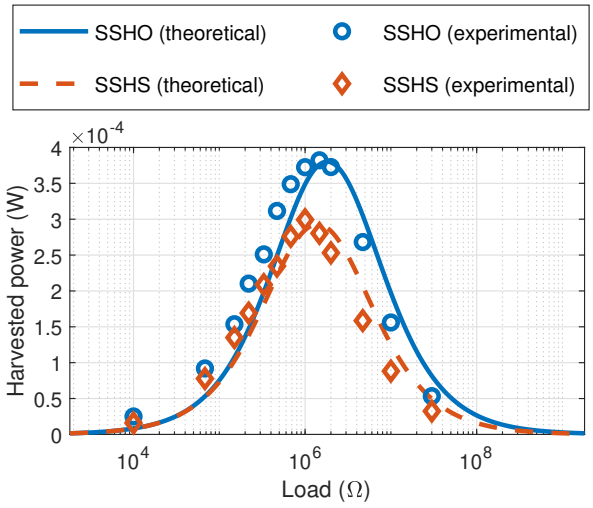

Fig. 9. Harvested power with SSHO and comparison with SSHS.

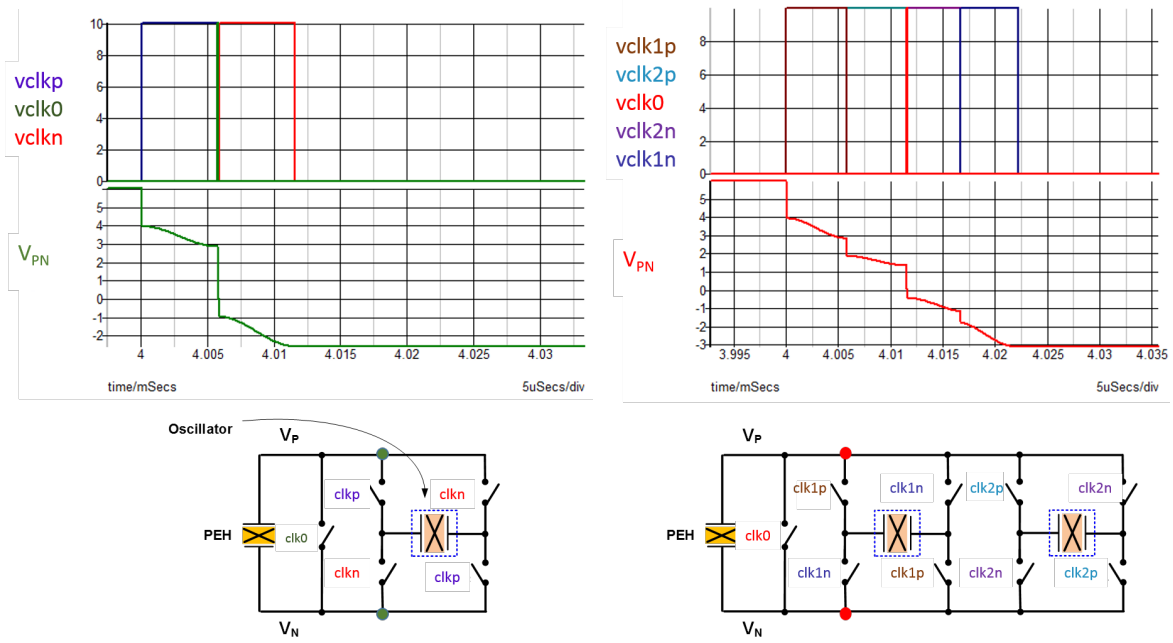

(a) 1 stage with charge cancellation (b) 2 stages with charge cancellation

Fig. 10. Preliminary simulations for multi-stage SSHO with charge cancellation.

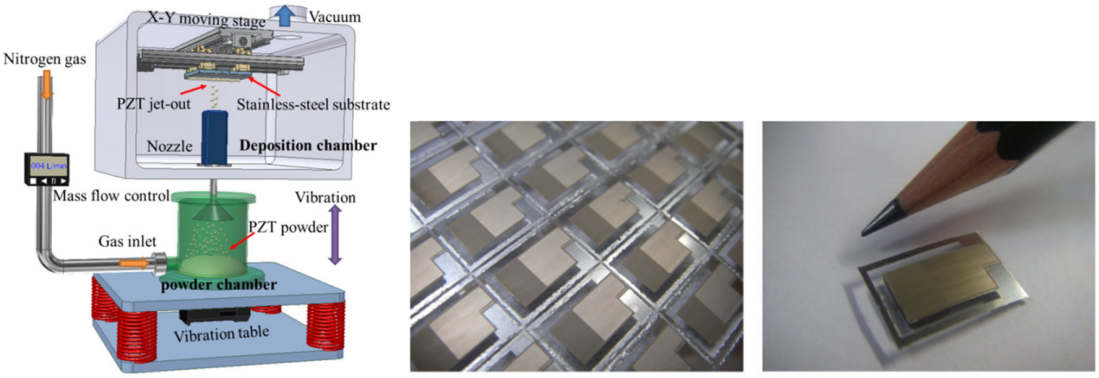

(a) Aerosol deposition equipment (b) Example of obtained sample

Fig. 11. Possibility for oscillator integration ([30]).

ACKNOWLEDGEMENTS

The authors gratefully acknowledge the support of Agence Nationale de la Recherche and Ministry of Science and Technology through respective grants $ANR-15-CE22-0015-01$ and $105-2923-E-002-006-MY3$ (BESTMEMS project). W.-J. WU also acknowledges the support of INSA through the invited professor program.

REFERENCES

[1] J. VanZwol, "Designing battery packs for thermal extremes", Power Electronics Technology , July 2006, pp. 4045, 2006.

[2] V. Knap, z D.-I. Stroe, M. Swierczynski, R. Teodorescu and E. Schaltz, "Investigation of the Self-Discharge Behavior of Lithium-Sulfur Batteries", J. Electrochem. Soc., Vol. 163 (6), A911-A916, 2016.

[3] M. A. Hannan, MD. M. Hoque, A. Hussain, Y. Yusof and P. J. Ker, "State-of-the-Art and Energy Management System of Lithium-Ion Batteries in Electric Vehicle Applications: Issues and Recommendations", IEEE Access, Vol. 6, pp. 19362-19378, 2018.

[4] X. Feng, M. Ouyang, X. Liu, L. Lu, Y. Xia and X. He, "Thermal runaway mechanism of lithium ion battery for electric vehicles: A review", Energy Storage Materials, Vol. 10, pp. 246-267, 2018.

[5] J. W. Matiko, N. J. Grabham, S. P. Beeby and M. J. Tudor, "Review of the application of energy harvesting in buildings", Meas. Sci. Technol., vol. 25, 012002, 2014.

[6] M. Q. Le, J.-F. Capsal, M. Lallart, Y. Hebrard, A. Van Der Ham, N. Reffe, L. Geynet and P.-J. Cottinet, "Review on energy harvesting for structural health monitoring in aeronautical applications", Progress in Aerospace Sci., vol. 79, pp. 147157, 2015.

[7] R. Md. Ferdous, A. W. Reza and M. F. Siddiqui, "Renewable energy harvesting for wireless sensors using passive RFID tag technology: A review", Renew. Sust. Energy Rev., vol. 58, 11141128, 2016.

[8] K. V. Selvan and M. S. M. Ali, "Micro-scale energy harvesting devices: Review of methodological performances in the last decade", Renew. Sust. Energy Rev., vol. 54, 10351047, 2016.

[9] F. K. Shaikh and S. Zeadally, "Energy harvesting in wireless sensor networks: A comprehensive review", Renew. Sust. Energy Rev., vol. 55, 1041-1054, 2016.

[10] G. D. Szarka, B. H. Stark and S. G. Burrow, "Review of Power Conditioning for Kinetic Energy Harvesting Systems", IEEE Trans. Power Elec., Vol. 27(2), pp. 803-815, 2011.

[11] N. Kong and D. S. Ha, "Low-Power Design of a Self-powered Piezoelectric Energy Harvesting System With Maximum Power Point Tracking", IEEE Trans. Power Elec., Vol. 27(5), pp. 2298-2308, 2012.

[12] Z. J. Chew and M. Zhu, "Adaptive Maximum Power Point Finding Using Direct VOC/2 Tracking Method With Microwatt Power Consumption for Energy Harvesting", IEEE Trans. Power Elec., Vol. 33(9), pp. 8164-8173, 2017.

[13] M. Lallart and D. J. Inman, "Low-Cost Integrable Tuning-free Converter for Piezoelectric Energy Harvesting Optimization", IEEE Trans. Power Elec., Vol. 25(7), pp. 1811-1819, 2010.

[14] Y. Tang and A. Khaligh, "A Multiinput Bridgeless Resonant AC-DC Converter for Electromagnetic Energy Harvesting", IEEE Trans. Power Elec., Vol. 31(3), pp. 2254-2263, 2015.

[15] Y. Sun, N. H. Hieu, C.-J. Jeong and S.-G. Lee, "An Integrated High-Performance Active Rectifier for Piezoelectric Vibration Energy Harvesting Systems", IEEE Trans. Power Elec., Vol. 27(2), pp. 623-627, 2012.

[16] J. Kim, J. Kim, M. Sim, S. Kim and C. Kim, "A Single-Input Four-Output (SIFO) ACDC Rectifying System for Vibration Energy Harvesting", IEEE Trans. Power Elec., Vol. 29(6), pp. 2629-2633, 2014.

[17] H. Wang, Y. Tang and A. Khaligh , "A Bridgeless Boost Rectifier for Low-Voltage Energy Harvesting Applications", IEEE Trans. Power Elec., Vol. 28(11), pp. 5206-5214, 2013.

[18] Y. Rao and D. P. Arnold, "An Input-Powered Vibrational Energy Harvesting Interface Circuit With Zero Standby Power", IEEE Trans. Power Elec., Vol. 26(12), pp. 3524-3533, 2011.

[19] G. W. Taylor, J. R. Burns, S. M. Kammann, W. B. Powers and T. R. Welsh, "The Energy Harvesting Eel: A Small Subsurface Ocean/River Power Generator", IEEE J. Ocean. Eng., vol. 26(4), pp. 539-547, 2001.

[20] D. Guyomar, A. Badel, E. Lefeuvre and C. Richard, "Toward Energy Harvesting Using Active Materials and Conversion Improvement by Nonlinear Processing", IEEE Trans. Ultrason. Ferroelec. Freq. Cont., vol. 52(4), pp. 584-595, 2005.

[21] E. Lefeuvre, A. Badel, C. Richard, L. Petit and D. Guyomar, "A comparison between several vibration-powered piezoelectric generators for standalone systems", Sens. Act. A: Phys., vol. 126, pp. 405-416, 2006.

[22] Y. C. Shu, I. C. Lien and W. J. Wu, "An improved analysis of the SSHI interface in piezoelectric energy harvesting", Smart Mater. Struct., vol. 16, 22532264, 2007.

[23] M. Lallart, L. Garbuio, L. Petit, C. Richard and D. Guyomar, "Double Synchronized Switch Harvesting (DSSH): A New Energy Harvesting Scheme for Efficient Energy Extraction", IEEE Trans. Ultrasonics, Ferroelec. Freq. Cont., Vol. 55(10): 2119-2130, 2008.

[24] H. Shen, J. Qiu, H. Ji, K. Zhu and M. Balsi, "Enhanced synchronized switch harvesting: a new energy harvesting scheme for efficient energy extraction", *Smart Mater. Struct.*, vol. 19(11), 115017, 2010.

[25] L. Garbuio, M. Lallart, D. Guyomar and C. Richard, "Mechanical Energy Harvester with Ultra-Low Threshold Rectification Based on SSHI Non-Linear Technique", IEEE Trans. Indus. Elec., Vol. 56(4), pp. 1048-1056, 2009.

[26] E. Lefeuvre, A. Badel, C. Richard and D. Guyomar, "Piezoelectric Energy Harvesting Device Optimization by Synchronous Electric Charge Extraction", J. Intell. Mat. Syst. Struct., vol. 16, pp. 865-876, 2005.

[27] Y. Wu, A. Badel, F. Formosa, W. Liu and A. Agbossou, "Piezoelectric vibration energy harvesting by optimized synchronous electric charge extraction", J. Intell. Mat. Syst. Struct., vol. 24(12), pp. 1445-1458, 2012.

[28] A. Romani, M. Filippi and M. Tartagni, "Micropower Design of a Fully Autonomous Energy Harvesting Circuit for Arrays of Piezoelectric Transducers", IEEE Trans. Power Elec., Vol. 29(2), pp. 729-739, 2014.

[29] M. Lallart, W.-J. Wu, Y. Hsieh and L. Yan, "Synchronous Inversion and Charge Extraction (SICE): a Hybrid Switching Interface for Efficient Vibrational Energy Harvesting", Smart Mater. Struct., Vol. 26(11), 115012, 2017.

[30] S. C. Lin and W. J. Wu, "Piezoelectric micro energy harvesters based on stainless-steel substrates", Smart Mater. Struct., vol. 22, 045016, 2013.

[31] W. H. Tang, T. K. Lin, C. T. Chen, Y. H. Fu, S. C. Lin and W. J. Wu, "A High Performance Piezoelectric Micro Energy Harvester Based on Stainless Steel Substrates", IOP Conf. Series: Journal of Physics: Conf. Series, Vol. 1052, 012038, 2018.

[32] Y. Zhang and D. Ma, "Input-Self-Biased Transient-Enhanced Maximum Voltage Tracker for Low-Voltage Energy-Harvesting Applications", IEEE Trans. Power Elec., Vol. 27(5), pp. 2227-2230, 2012.

[33] J. Brufau-Penella and M. Puig-Vidal, "Piezoelectric Energy Harvesting Improvement with Complex Conjugate Impedance Matching", J. Intell. Mat. Syst. Struct., Vol. 20(5), pp. 597608, 2009.

[34] S. Du and A. A. Seshia, "An Inductorless Bias-Flip Rectifier for Piezoelectric Energy Harvesting", IEEE J. Solid-State Circ., Vol. 52(10), pp. 2746-2757, 2017.

[35] W. J. Wu, A. M. Wickenheiser, T. Reissman and E. Garcia, "Modeling and experimental verification of synchronized discharging techniques for boosting power harvesting from piezoelectric transducers", Smart Mater. Struct., vol. 18, 055012, 2009.

[36] Z. Chen, M.-K. Law, P.-I. Mak, W.-H. Ki and R. P. Martins, "Fully Integrated Inductor-Less Flipping-Capacitor Rectifier for Piezoelectric Energy Harvesting", IEEE J. Solid-State Circ., Vol. 52(12), pp. 3168-3180, 2017.

[37] Z. Chen, M.-K. Law, P.-I. Mak, W.-H. Ki and R. P. Martins, "A 1.7mm^2 inductorless fully integrated ipping-capacitor rectier (FCR) for piezoelectric energy harvesting with 483% power-extraction enhancement", Proc. 2017 IEEE International Solid-State Circuits Conference (ISSCC), 5-9 Feb. 2017, San Francisco, CA, USA, p. 372.